Chapter 7

Prestack Migration Examples

This chapter is devoted to assessing the quality and usability of a wide variety of prestack imaging algorithms. Visual side-by-side comparisons provide ample empirical evidence to conclude that the more accurate the algorithm, the wider the aperture, and the more careful the application, the better the result. Ultimately, we will argue that the full two-way method is by far the best at providing optimum imaging. When computational expense is not an issue, this should definitely be the method of choice.

The images in this chapter are self-explanatory and require little or no real attention to visual detail. Because they are so small, it is better to see them on the screen.

Common Azimuth on the SEG/EAGE C3-NA Synthetic

Figure 7-1, after Biondi *et al.*, represents a direct comparison between a Kirchhoff migration and a full one-way common azimuth migration.

Figure 7-1. Common azimuth versus a single arrival Kirchhoff migration of the SEG/EAGE C3-NA data volume.

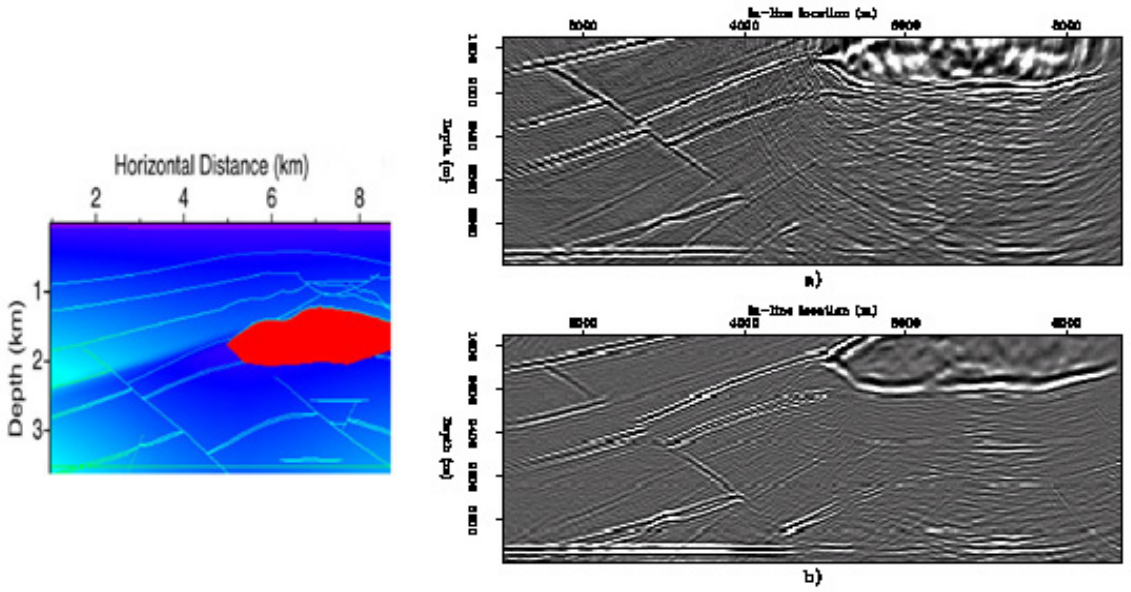

Kirchhoff versus One-Way on a Gulf of Mexico 2D Salt Synthetic

This short section looks at a major reason we should use highly accurate imaging techniques. It compares a one-way phase screen to a maximum amplitude Kirchhoff method. Improvements at both the salt-sediment interface and below the salt provide clear evidence of the superiority of the more accurate one-way technique.

A series of widely spaced shots were synthesized over the model shown in the upper right corners of both halves of Figure 7-2. Receivers for each shot were spread across the entire model surface. The one-way technique clearly does a better job overall and is much better at the salt-sediment interface and in the sub salt section of the model.

Figure 7-2. A comparison of Kirchhoff and one-way migrations Algorithms.

(a). Model and prestack Kirchhoff migration **(b).** Model and one-way phase screen

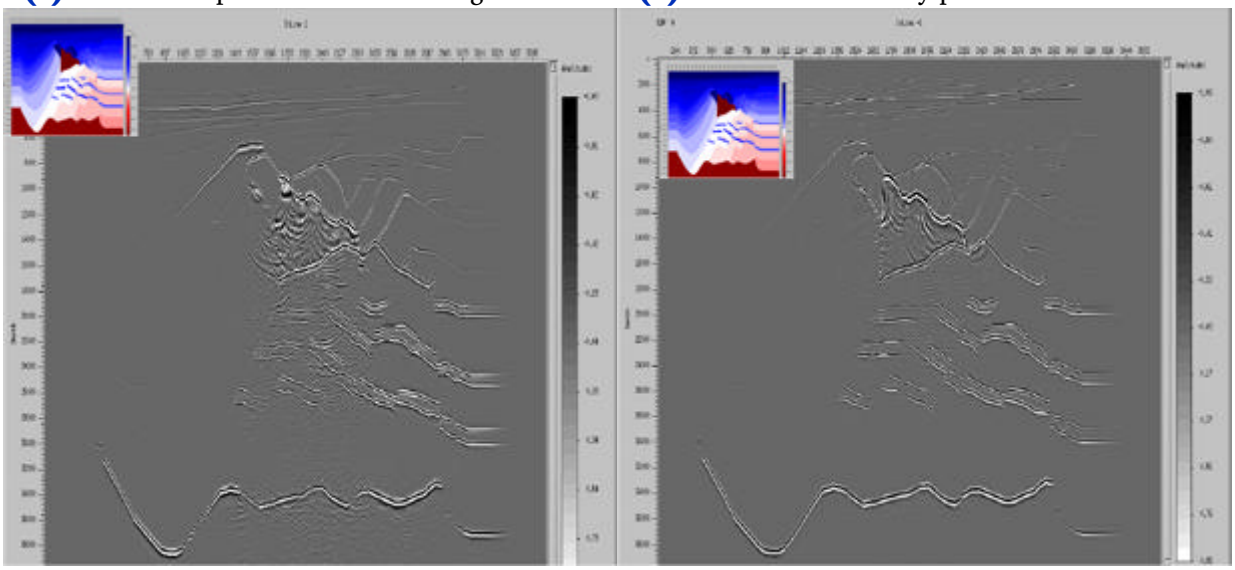

A North Sea Sill Synthetic

The model in Figure 7-3 was designed by Dr. Rob Hardy at Trinity University in Dublin, Ireland. The synthetic data were generated using Panorama Technologies advanced finite difference modeling technology. All images in this figure were based on the same input data. The Kirchhoff image was the result of an application of Seismic Unix's Kirchhoff migration from the Colorado School of Mines.

Figure 7-3. Volcanic Sills Model and Migrated images

(a). Volcanic Sills Model

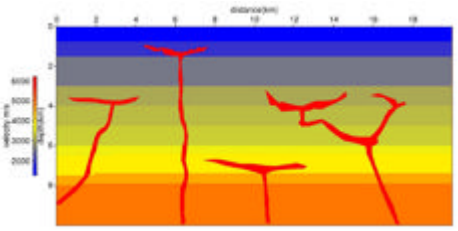

(b). SU Kirchhoff of the Sills Data

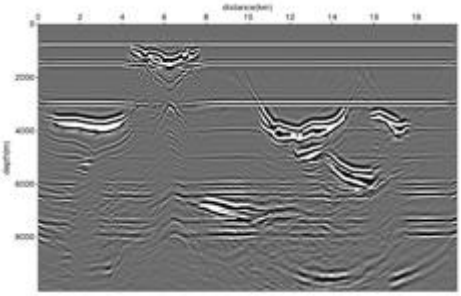

(c). One-way FKX image of the Sills Data

(d). Two-way XT image of the Sills Data

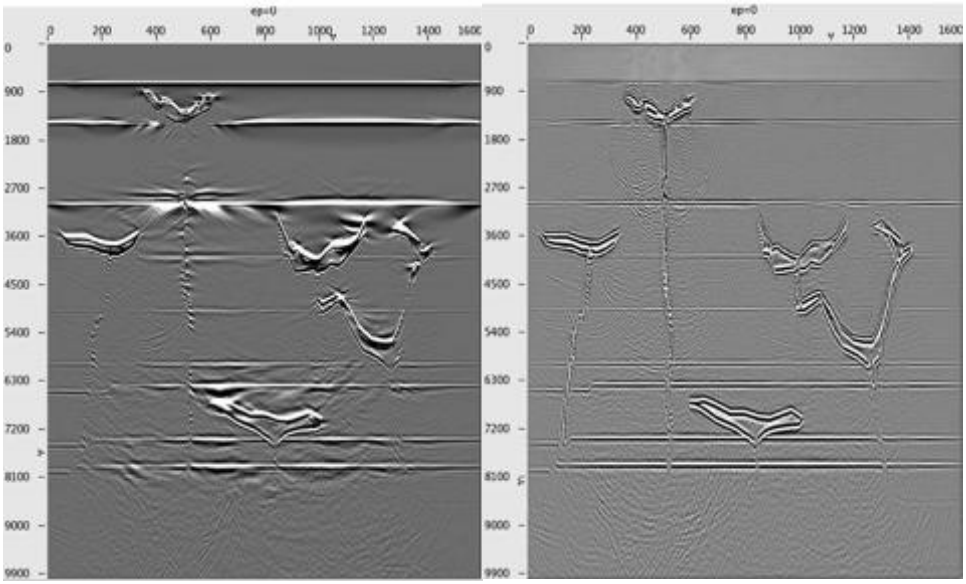

Marmousi Case Study

The Marmousi data set was generated under the direction of Roloff Versteeg (1990), while at the Institute de Francis du Petrol (IFP) in Paris, France. The velocity or Earth model is based on an actual prospect from offshore Western Africa. The Marmousi data have proven to be a gold mine for both development of imaging algorithms and for showing practitioners of the art that the world is not as simple as they originally thought. Here we see that problems with Kirchhoff techniques are not strictly limited to Gulf of Mexico style salt structures.

The various parts of Figure 7-4 are self-explanatory. The only conclusion we can reach is that multi-arrival methods are absolutely necessary to ensure optimum imaging. In the author's mind, the full two-way image in the lower right corner (Figure 7-4(f)) is superior to all the others, but at least three of the other methodologies would give satisfactory results for exploration purposes.

Figure 7-4. A comparison of prestack algorithms on the Marmousi data set.

(a). The Marmousi velocity model

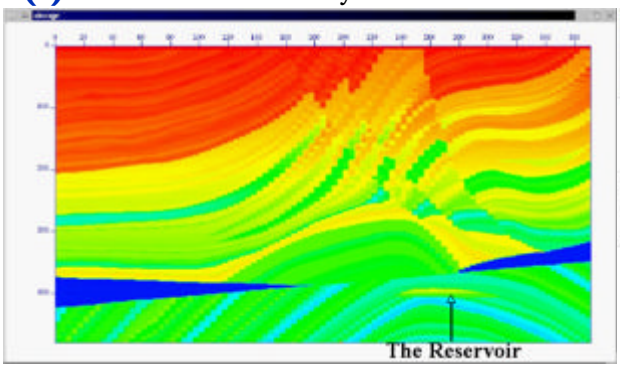

(b). Multi arrival Kirchhoff after Sam Gray Veritas

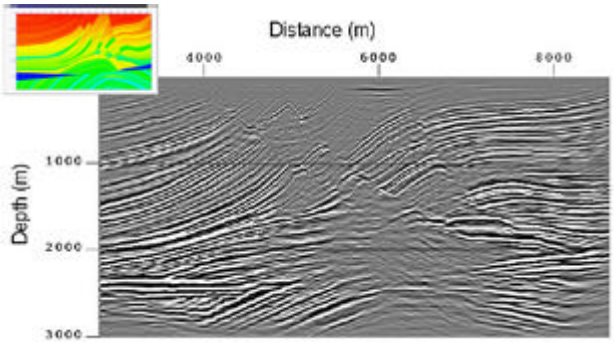

(c). Gaussian Beam after Hill 2001

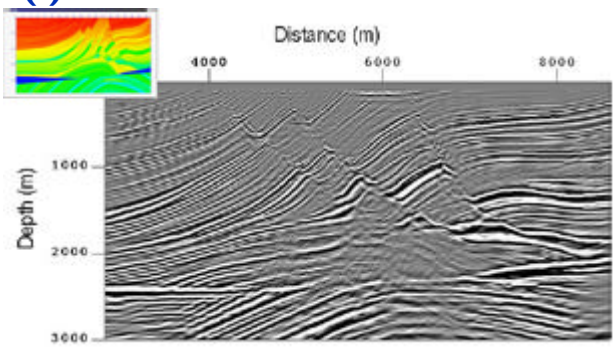

(d). Single arrival Kirchhoff migration

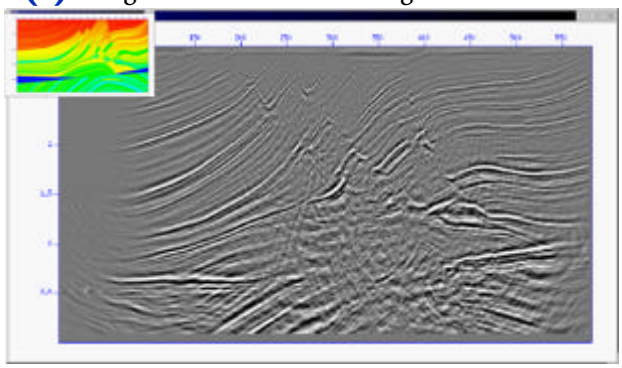

(e). One-way phase screen migration

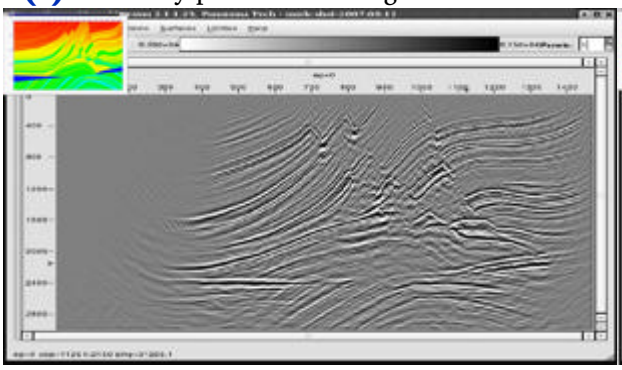

(f). Full two-way finite difference migration

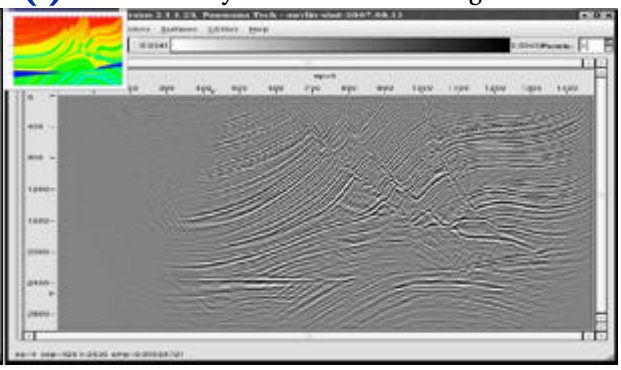

An Imaging Note and the BP 2.5 Dimensional Data

Before providing some comparisons of one- and two-way migrations on complex data sets, it is worth discussing imaging data sets that, because of severe illumination or surface issues, might have wide ranging differences in both source generated and receiver suppressed energy levels. This issue was brought to light by several researchers at AMOCO and later BP. J. T. Etgen, Carl Regone and colleagues generated the model, which, when migrated, produced such a wide range of output reflection strengths that just displaying it was difficult.

Figure 7-5 shows how this reflection strength disparage can be overcome by a careful compensation for illumination. The bottom part of this figure shows a straightforward migration of the original input data. The middle part represents the illumination in space and depth. Simply dividing by this quantity produces the image at the top of Figure 7-5. Note that this process is not equivalent to an automatic gain control. It is actually based on being able to correctly handle energy differences specified by the Earth model and correct the output image for lateral and vertical differences.

Figure 7-5. Using illumination corrections to properly gain imaged data.

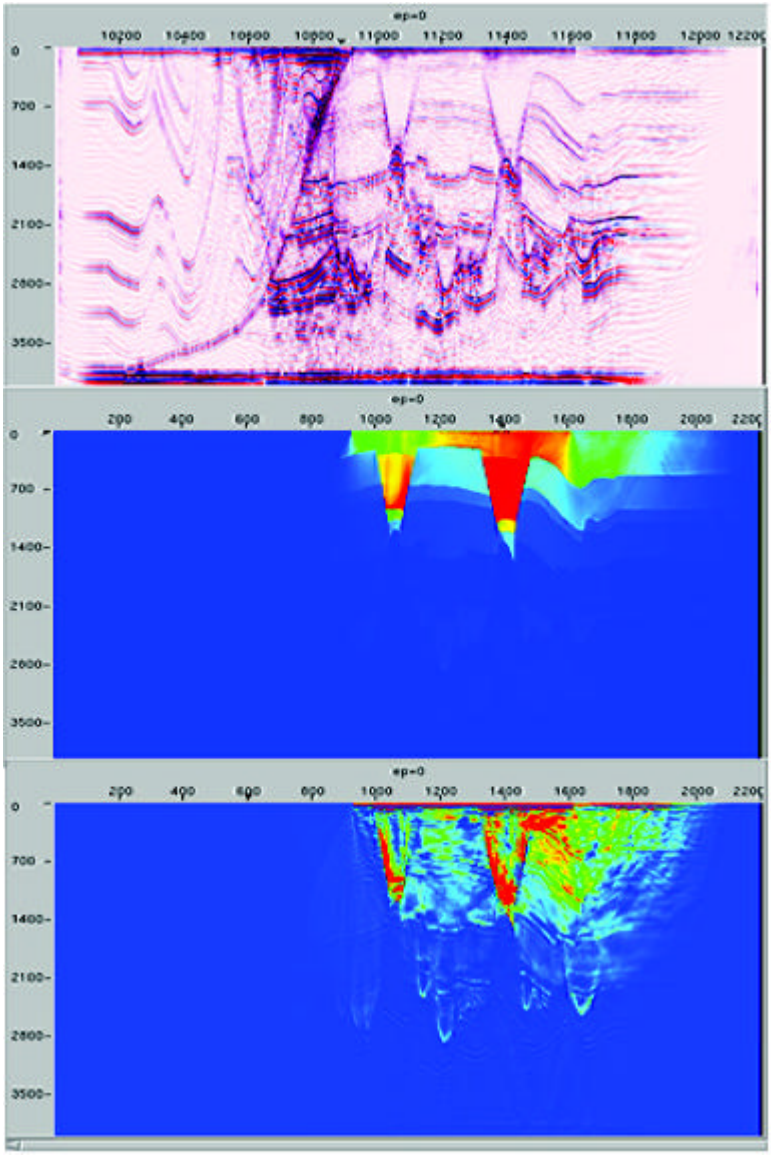

BP 2.5 D Data

Each graphic in Figure 7-6 represents application of either a one-way or a two-way method to the original BP 2.5D data set. Parts (a) and (b) show an image of the velocity model overlaid on a one-way image of the raw input data along with the one-way image without the overlay. Parts (c) and (d) show the need to properly account for differences in both illumination and energy spreading losses. Parts (e) and (f) show that use of a well implemented imaging condition can produce dramatic results.

Figure 7-6. Imaging with proper illumination correction.

(a). One-way BP 2.5D data with velocity overlay

(b). Two-way BP 2.5D data without illumination

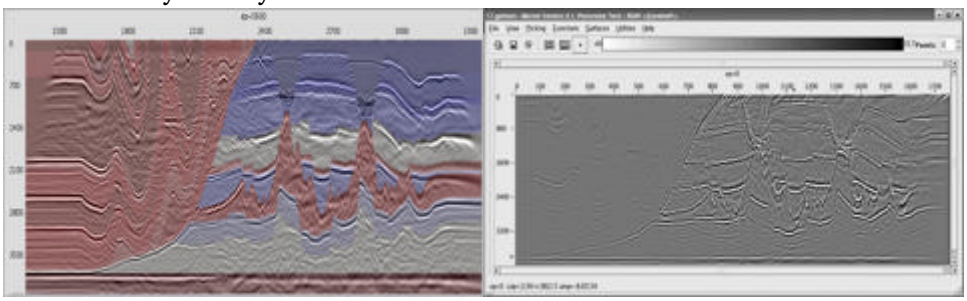

(c). Two-way BP 2.5D data with normal imaging

(d). One-way BP 2.5Dl data with overlay

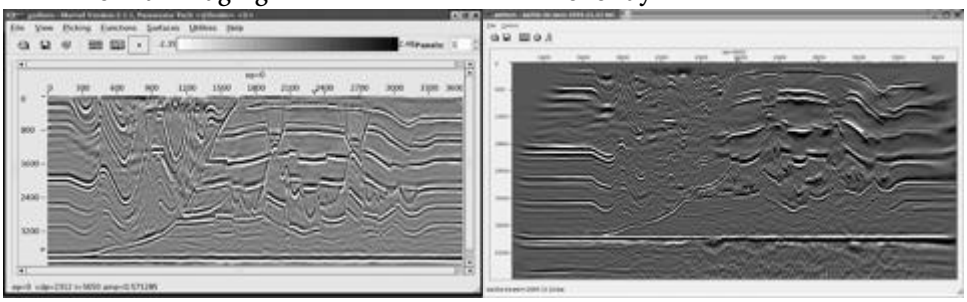

(e). Two-way BP 2.5D data with illumination

(f). Two-way BP 2.5D with optimum imaging

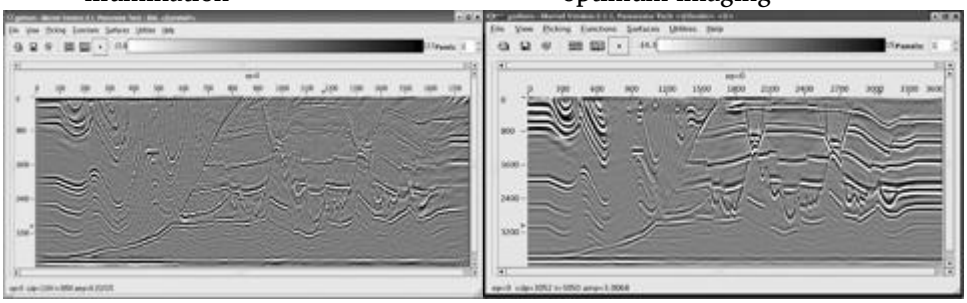

BP 2004 Salt Structure Data

Figure 7-7(a) is a graphic of the velocity model for the Earth model used to generate realistic data for evaluation of imaging techniques. This model is very complex, with lateral velocity ratios close to 2:1 at many depth levels. Part (b) of this figure compares two partial images. The image on the left in part (b) was obtained from a one-way method, while the image on the right is a two-way image using exactly the same parameters and input data. Clearly, the two-way method images much more of the subsurface than does the one-way method. This is very likely because the two-way method produces a much more accurate impulse response at all angles. Part (c) shows that the two-way method can provide an excellent response even without multiple suppression.

Figure 7-7. Migration of the complex BP2004 data.

(a). BP 2004 Model after F. Billette

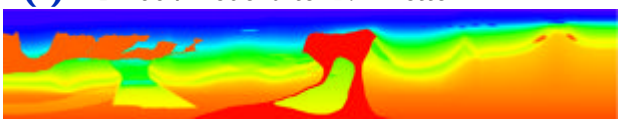

(b). One-way versus two-way on the same input data

(c). Full two-way migration on the BP 2004 data volume

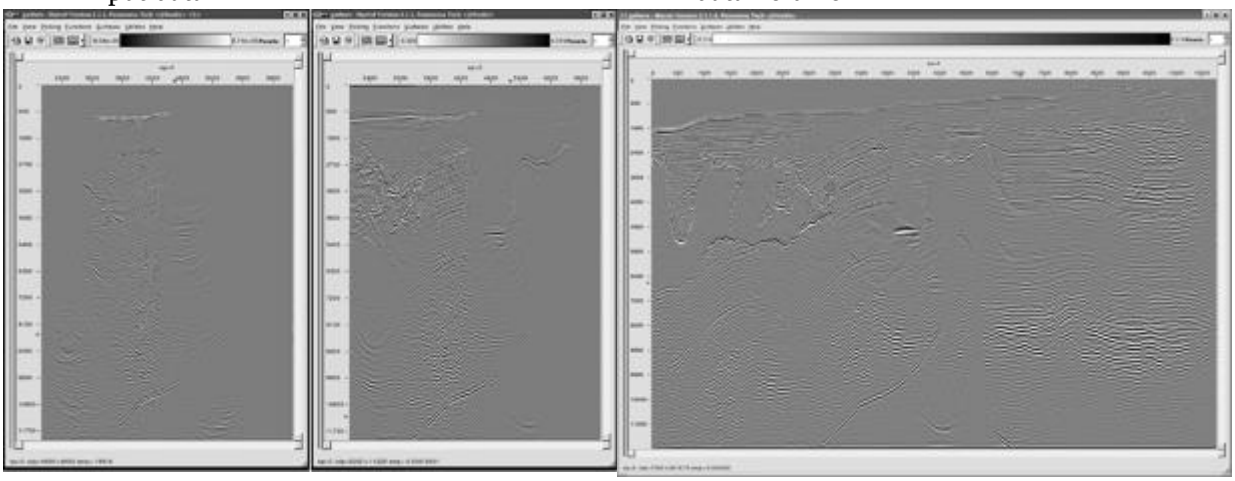

SEG AA′ Data Set

The SEG AA′ data set was originally a test 2D data set shot over a selected line from the full SEG/EAGE model. It has been said (personal communication from Sam Gray) that almost any algorithm can be made to image this data set reasonably well. Here, we simply compare a one-way split step method to a more accurate full two-way method.

Figure 7-8(a) is the original SEG AA′ velocity model. Figure 7-8(b) is an image of the prestack data originally shot over this model at AMOCO production before it became part of BP. Part (b) is a two-way image of this data, and is clearly better than the one-way result.

Figure 7-8. SEG AA′ model and associate one and two-way images.

(a). The SEG AA′ velocity model

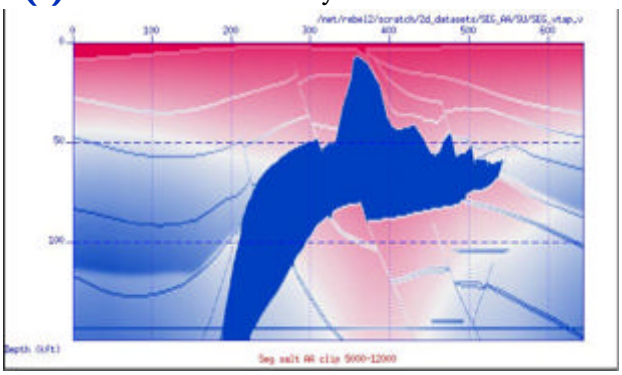

(b). One-way image of the AA′ data

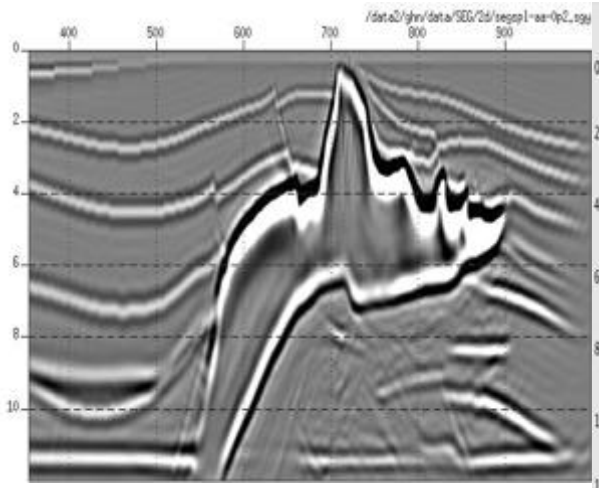

(c). Two-way image of the AA′ data

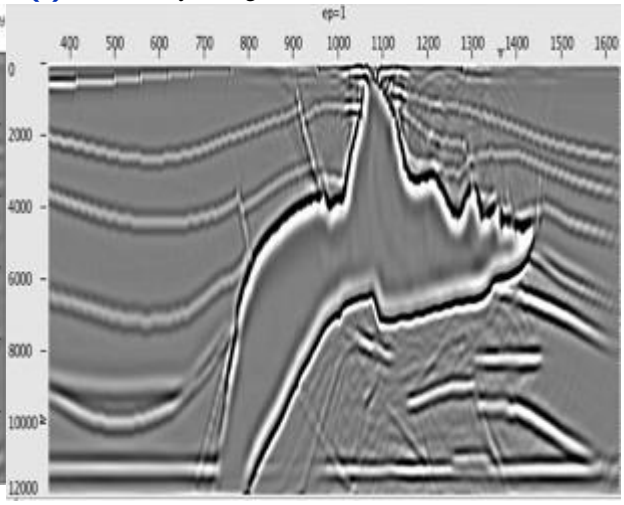

Migration from Topography

The traditional approach to handling data taken in areas of extreme (or even modest) topography is to statically correct the data to some datum, and then migrate as if the source and receivers were on the usually absolutely flat plane. It is quite easy to perform the migration directly from the topography. The major difficulty is not in making the algorithm handle the topography, but, instead, the difficulty arises in having accurate topographic data available and in being able to estimate an accurate near surface velocity field. What this section shows is that migrating from topography is not an issue.

Migration from topography requires the exact specification of the location and elevation of each and every source and receiver in the acquisition. Even though this information is routinely available, it is frequently not stored concomitant with the data, or it is lost after static corrections. Implementation of migration from topography requires only that wavefields be generated at the source or back-propagated from the receiver locations and elevations. Part (a) of Figure 7-9 shows a relatively simple model with relatively complex topography. Parts (b) and (c) show Kirchhoff and two-way images of these data. Visual comparison suggests that, again, the two-way approach is vastly superior to the Kirchhoff method.

Figure 7-9. Migration from topography.

(a). The BP (AMOCO) Canadian foothills topographic model

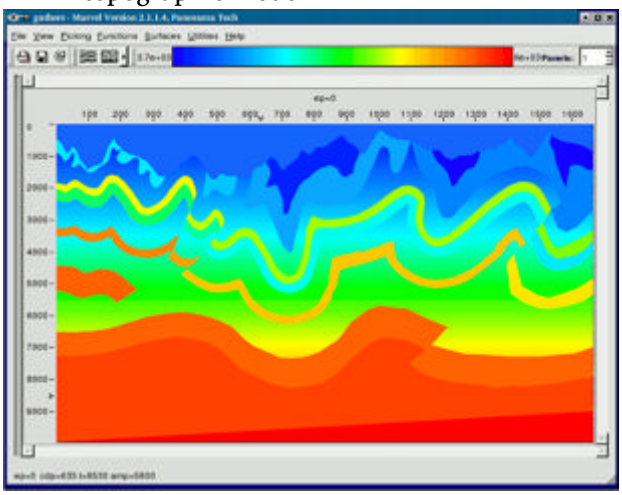

(b). Kirchhoff migration of the BP tomographic data

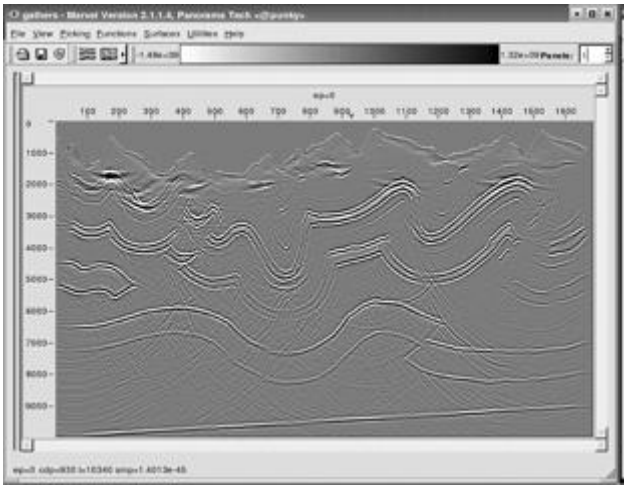

(c). Full wavefield migration of the BP tomographic data

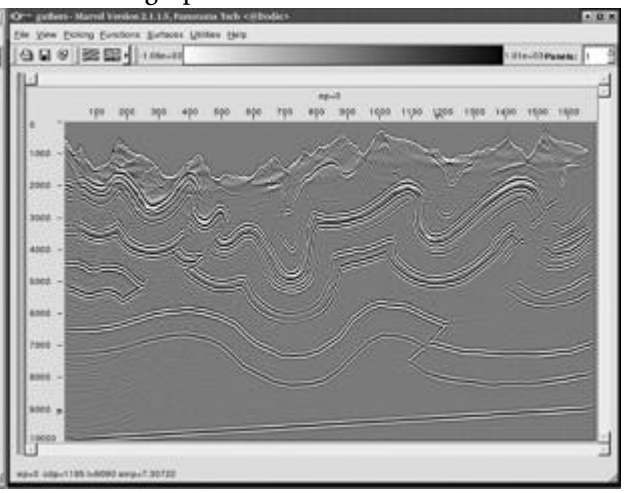

The SMAART JV Sigsbee Model

The SMAART JV (Subsalt Multiples Attenuation And Reduction Team Joint Venture) was an industry-sponsored joint venture focused on designing realistic Earth models and acquiring data over them to test the then current methodologies for imaging and multiple suppression. The first of the two images in Figure 7-10 shows the model used to synthesize the data as well as several images of the synthetic data. What is most interesting is the excellent amplitude response of the two-way algorithm.

Figure 7-10 shows the Sigsbee model in part (a), a Kirchhoff vertically varying gained image in part (b), a one-way image with no gain in part (c), and a full illumination corrected two-way image in part (d). The two-way image shows outstanding amplitude restoration and, in fact, when compared to the model in part (a), provides an excellent image proportional to reflectivity.

Figure 7-10. Sigsbee model and images from the SMAART Joint Venture project

(a). SMAART JV Sigsbee salt model

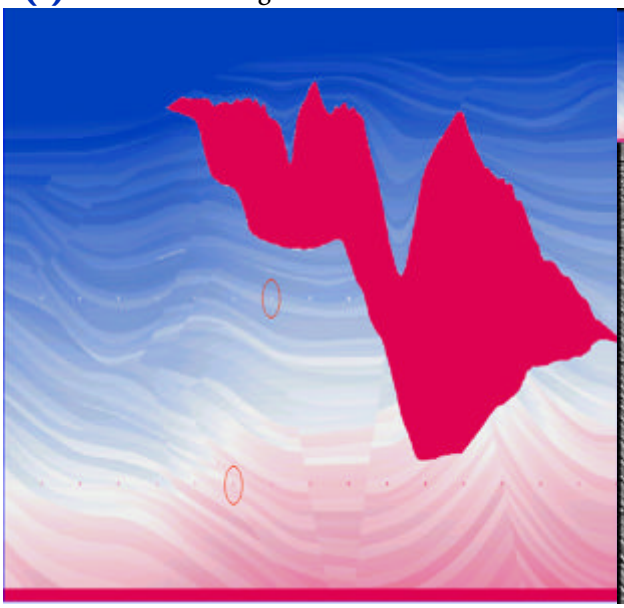

(b). Kirchhoff image (Sam Gray et. al)

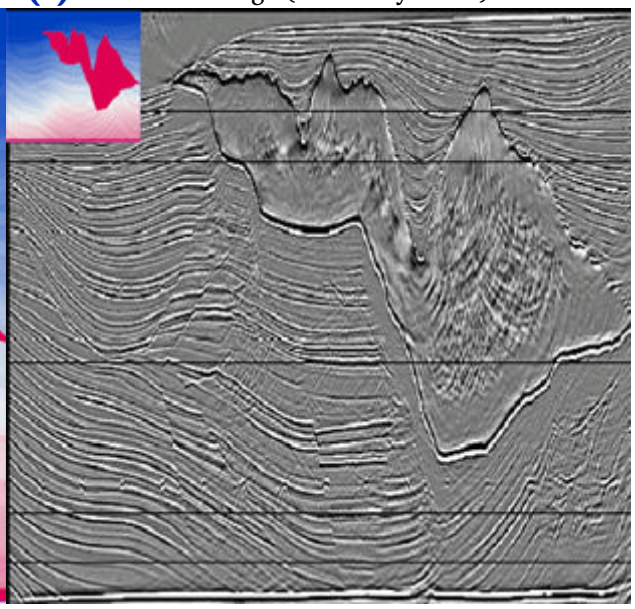

(c). One-way image

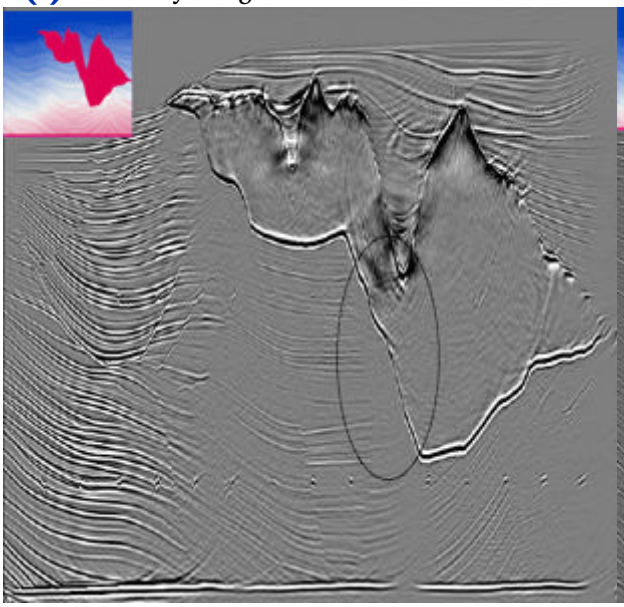

(d). Two-way image

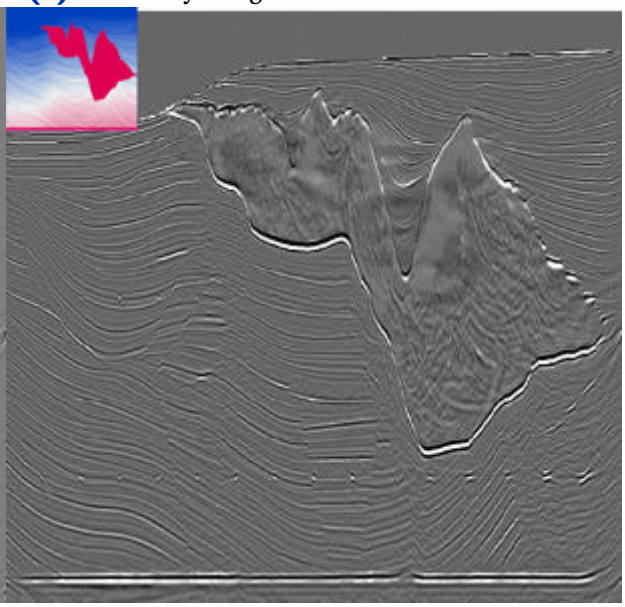

The zoomed images in Figure 7-11 that came from the original images in Figure 7-10 confirm the much higher quality imaging capabilities of two-way methodology.

Figure 7-11. Zoomed images from Figure 7-10

(a). Zoom comparison of one-way on the left and two-way on the right

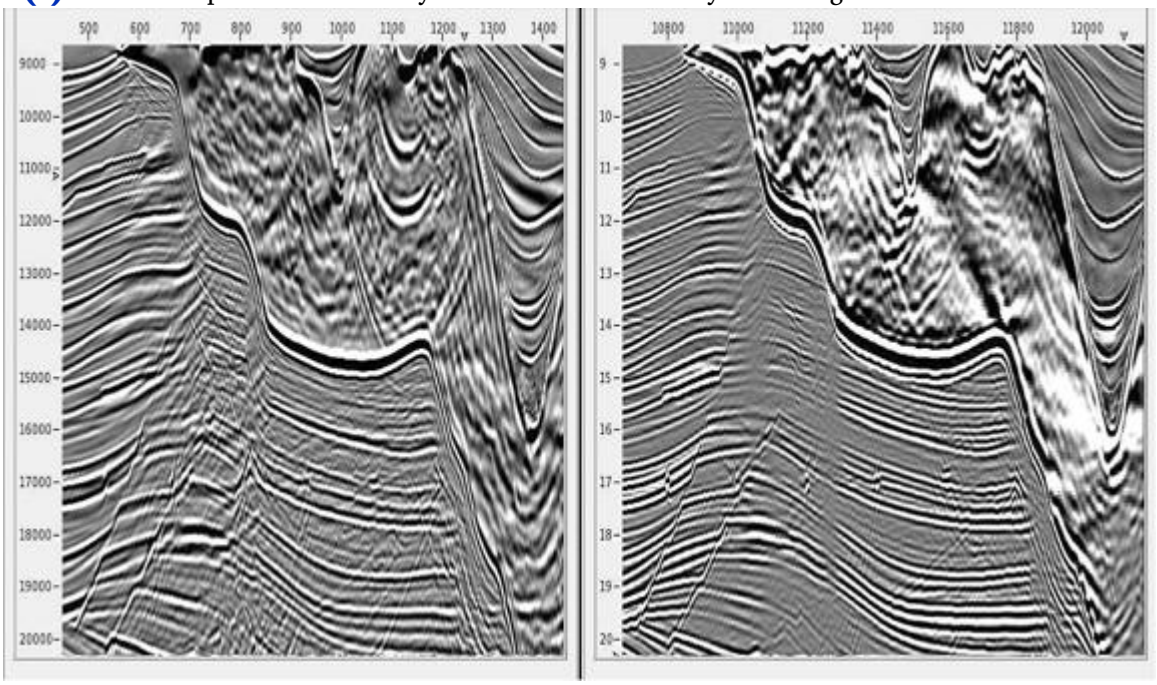

(b). Zoom comparison of one-way on the left and two-way on the right

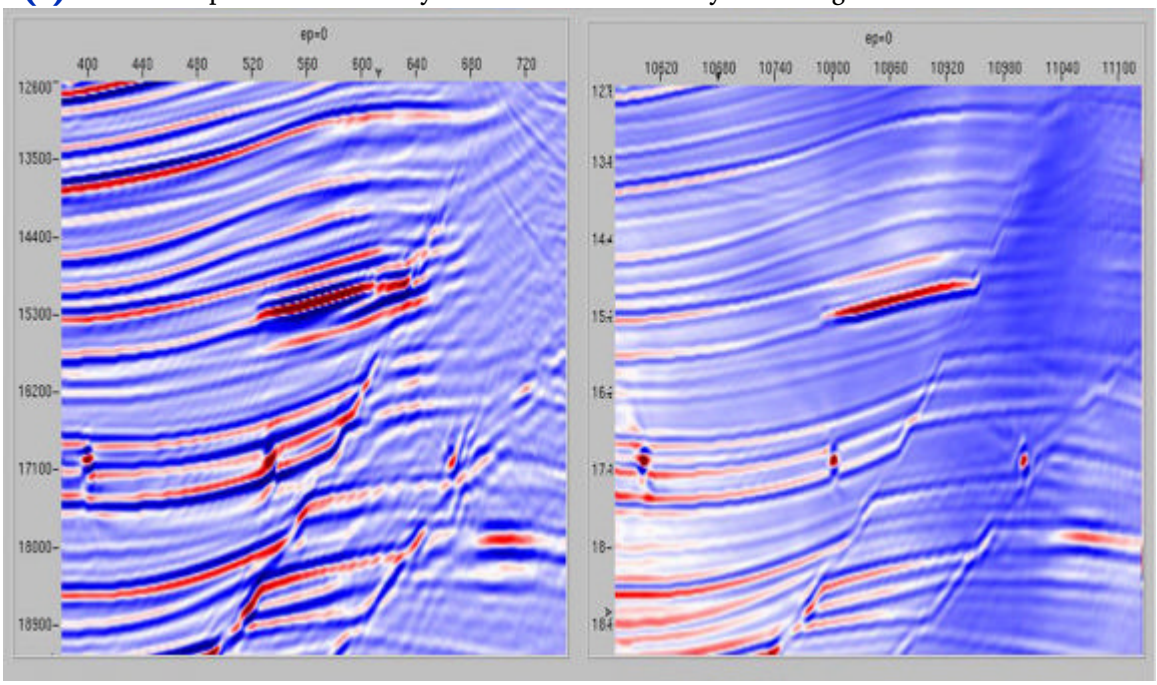

SMAART JV Pluto Data Set

In addition to designing and synthesizing data over a complex salt model, the SMAART JV data sets also produce data over a model designed specifically to test surface-related multiple elimination (SRME) algorithms. The Pluto data set is somewhat unusual because it contains a full set of zero-offset traces.

The images in Figure 7-12 visually quantify the impact of multiple energy on the higher technology migration algorithms. Part (a) provides a glimpse of the impact of multiples on a one-way phase screen migration of the Pluto data. Part (b) shows improved results when the multiples have been suppressed by SRME, but the two-way image in (c) is a better image still, even though it was produced with only 50% of the input data.

Figure 7-12. SMAART JV Pluto data set images.

(a). One-way migration with no SRME

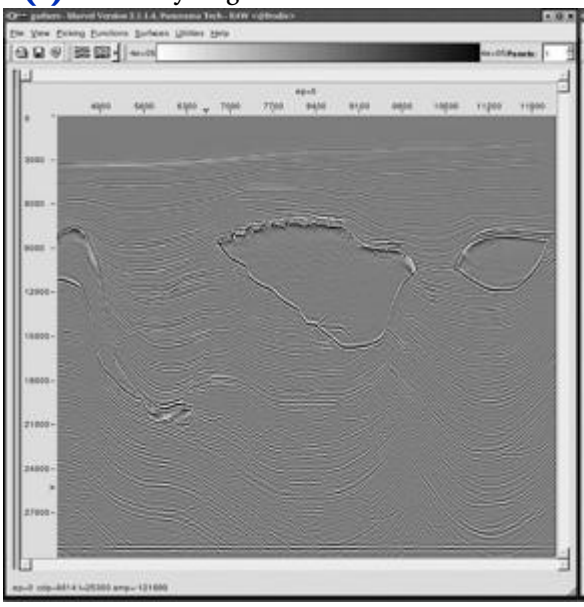

(b). One-way migration with SRME

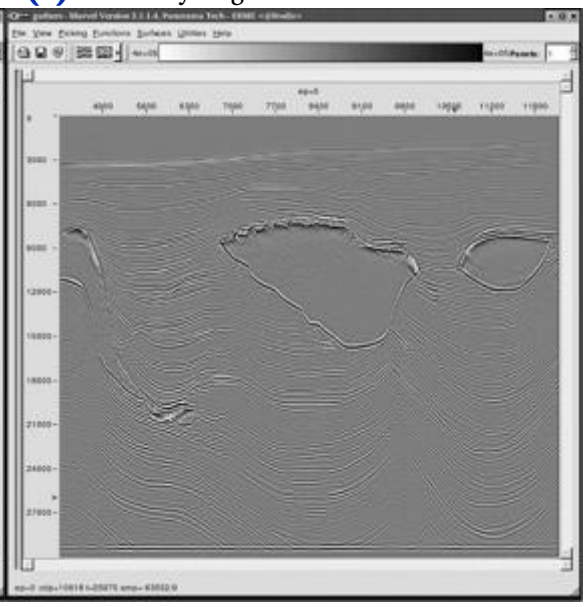

(c). Two-way image of 50% of the input data

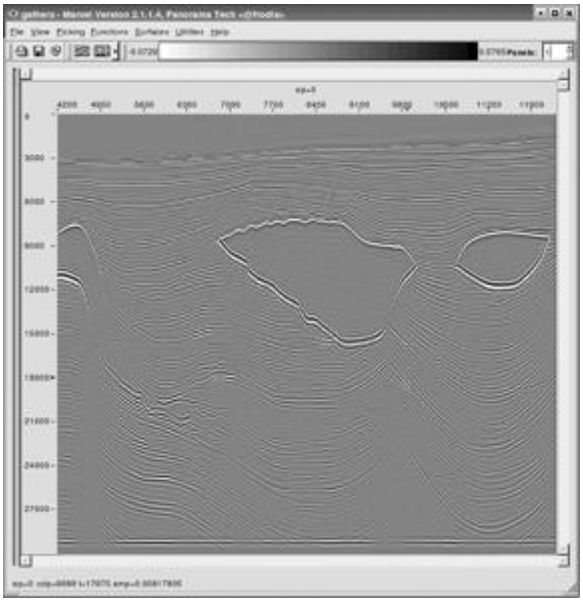

SEG/EAGE C3-NA Data Imaging

In this section, we consider the question of why imaging below salt for the C3-NA data set is so difficult

The two-way migration of the SEG/EAGE salt data represented in Figure 7-13(a) and (b) is quite good and compares favorably with the one-way migration in the left hand side of Figure 7-13(c). However, it is quite clear that, in spite of the excellent imaging, neither method provides a satisfactory image below salt.

Figure 7-13. SEG/EAGE C3-NA salt images

(a). A 3D two-way image

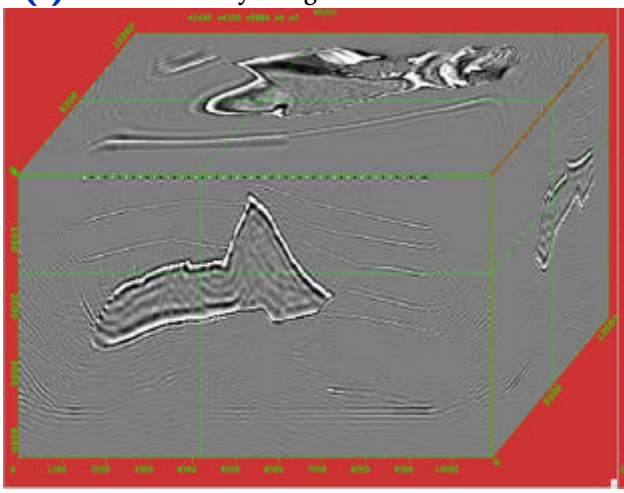

(b). A 3D two-way image

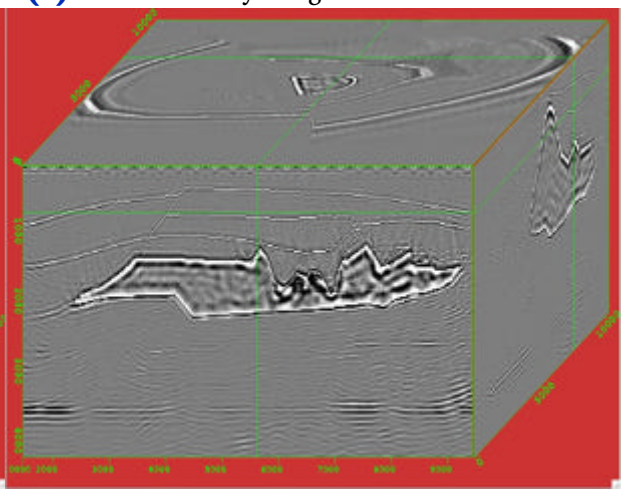

(c). A comparison one-way and two-way on Line 289

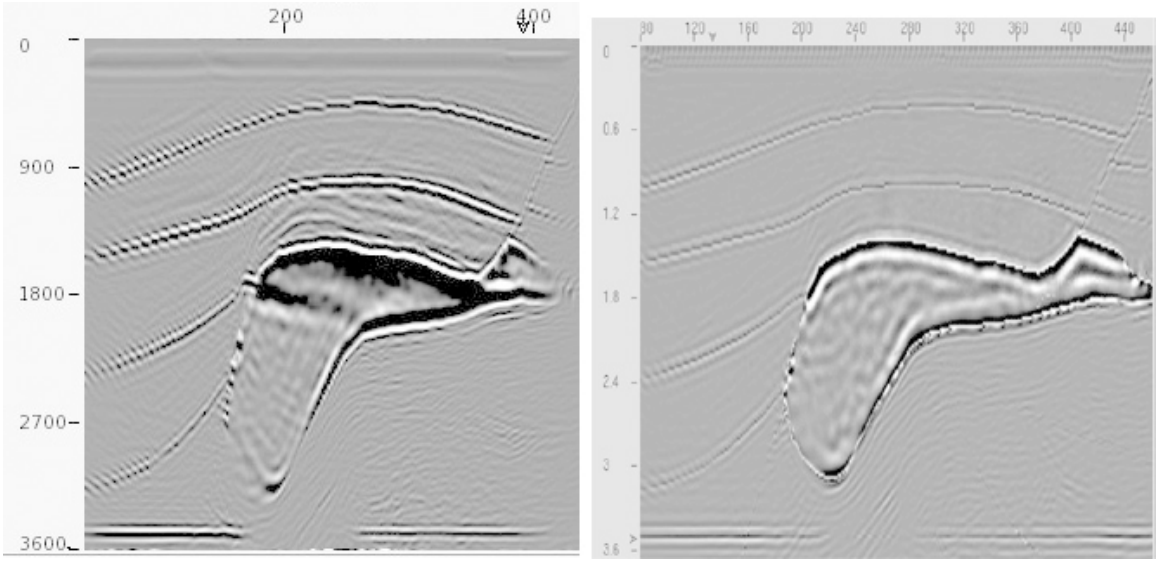

Figure 7-14 shows the result of proper data acquisition. The model in part (a) was used to synthesize densely spaced shots with apertures that covered the entire model. These data were then migrated to produce the image in parts (b) and (c). The graphic in part (b) of this figure is an excellent image of the sub salt reflectors. The same is true for the two-way image in part (c). The only possible conclusion is that proper acquisition is required for optimum imaging.

Figure 7-14. Imaging below salt

(a). A 2D line extraction from the 3D SEG/EAGE salt model

(b). One-way image of a 2D acquisition over the model in (a)

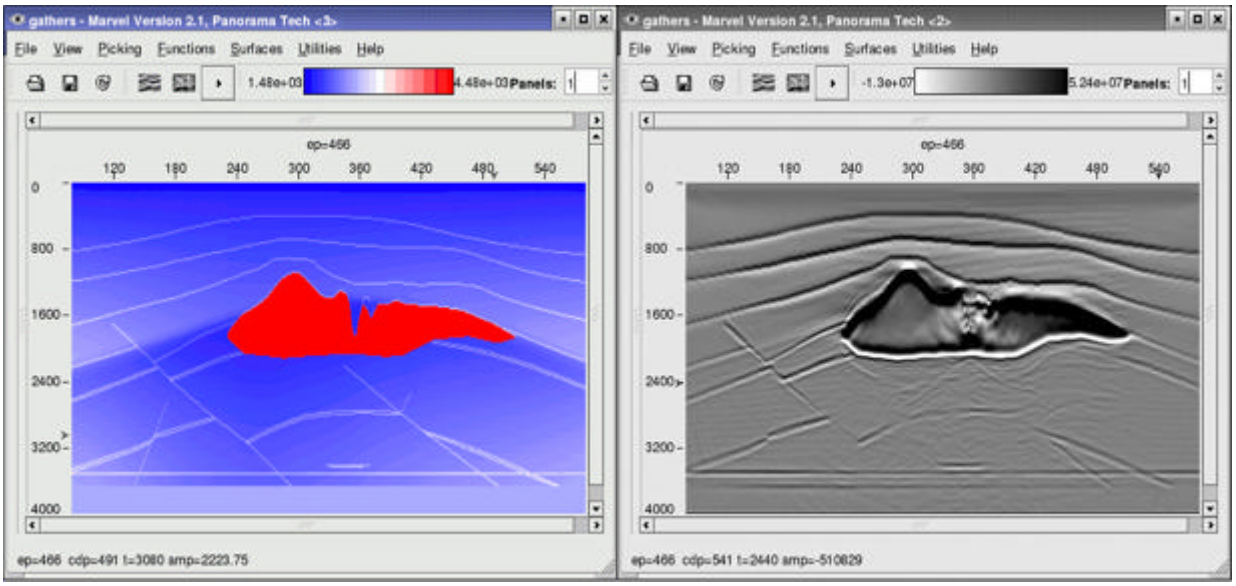

(c). Two-way image of a 2D acquisition over the model in (b)

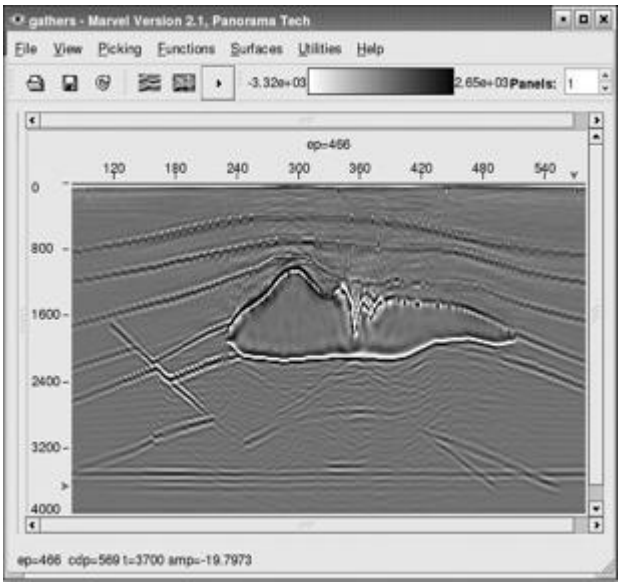

Anisotropic Earth Models

This section provides a simple example of how even simple anisotropic migrations can bring improved imaging to the migration arena. The Earth model in this section is based on an actual exploration problem that arose when drilling revealed a structure that was not apparent in the original imaging exercise. The vertical or well velocity of the highlighted turtle-like structure in the center of the model does not change. It is only the horizontal or NMO velocity that indicates its presence.

Figure 7-15 is an example of a simple 2D anisotropic Earth model. Shown are the vertical or well velocity (top left), the NMO velocity (top right), Thomsen's parameter δ (bottom left), and Thomsen's parameter η (bottom right).

Figure 7-15. An anisotropic Earth Model.

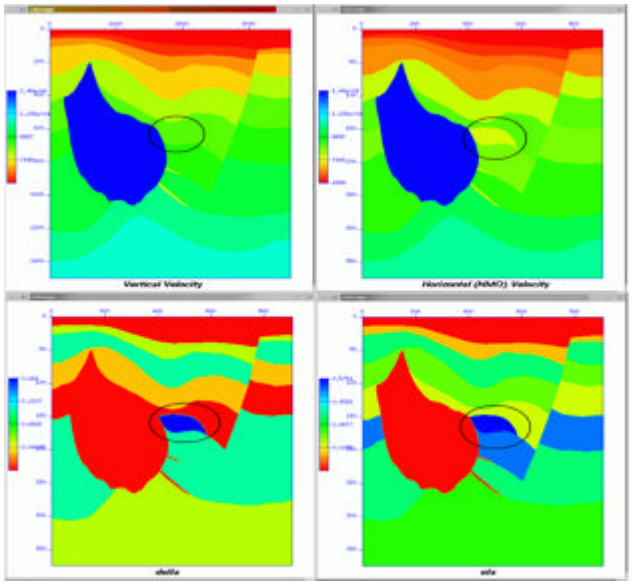

Although this figure contains four graphics, such models can be represented by only three parametric volumes. Given a vertical velocity, V_v, and Thomsen's parameters, δ and ε, we can express any of the others by suitable rearrangement of Equation 7-1 and Equation 7-2.

(7-1) $$V_{NMO} = V_v\sqrt{1+2\delta}$$

(7-2) $$\eta = \frac{\varepsilon - \delta}{\sqrt{1+2\delta}}$$

From a practical perspective, we usually estimate V_{NMO} using what has become traditional Kirchhoff based migration velocity analysis.

Since

(7-3) $$\delta = .5\frac{V_{NMO}}{V_v} - .5$$

it is clear that δ can be estimated through a simple combination of a well velocity and a velocity volume estimated through the usual migration velocity analysis process. Unfortunately, the same cannot be said for ε.

Figure 7-16 shows a set of images from several experiments to determine the extent to which anisotropic imaging might be of value.

Figure 7-16. Isotropic versus Anisotropic Imaging

(a). Isotropic with vertical velocity (left) and NMO (right)

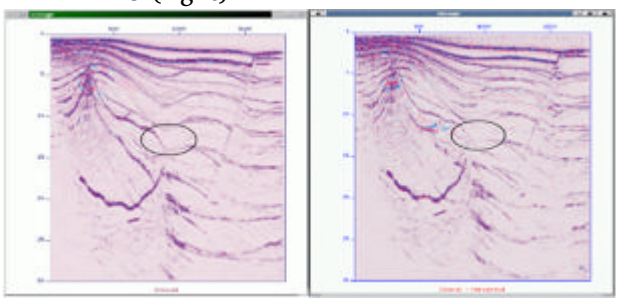

(b). Zoom of (a)

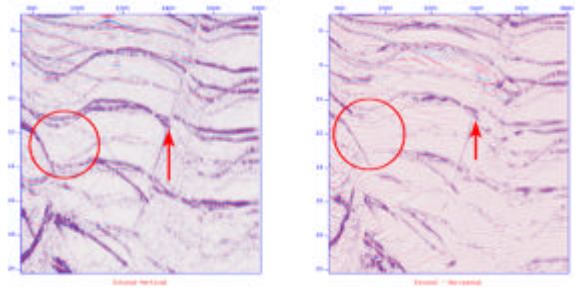

(c). Shot versus Eikonal

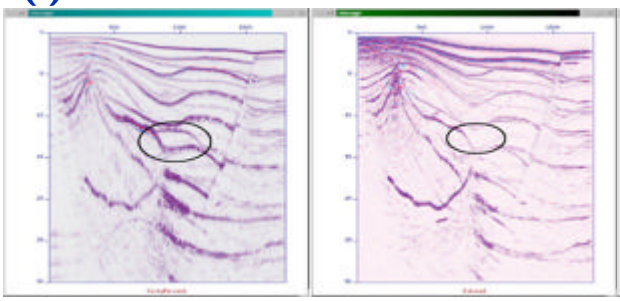

(d). Shot (left) versus Anisotropic Kirchhoff (right)

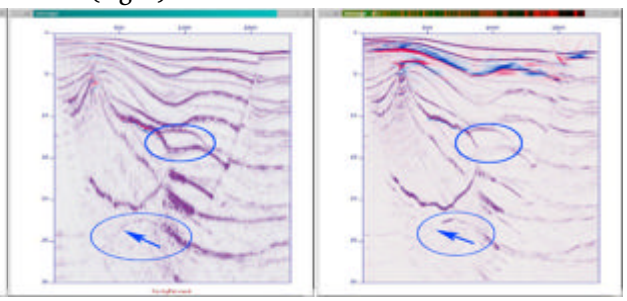

(e). Zoom of (d)

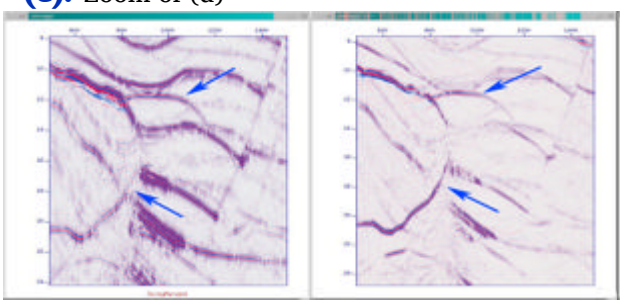

(f). Anisotropic (left) versus Isotropic (right) CDPs

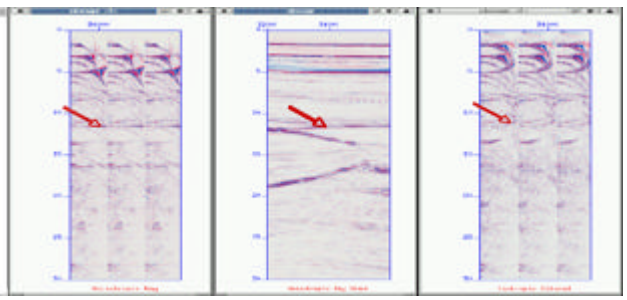

For this purpose, the model in Figure 7-15 was used to generate a series of shots. Figures 7-16(a) through (g) are various comparisons using different combinations of the underlying Earth model derived from that in Figure 7-15. Figure 7-16(a) and (b) show the results of using either the well velocity or the NMO velocity alone. The turtle back structure in these figures is essentially invisible so there is no reason to suspect its existence. While use of the vertical velocity does produce reasonable depth conversion when the reflecting horizon is relatively flat, steeply dipping events are either not imaged or are misplaced. Use of the NMO velocity tends to get steeply dipping events in their proper place, but does a poor job of depth conversion.

As shown in Figures 7-16(c) and (d), the issue changes quite quickly when an isotropic shot using the vertical velocity, or a full Kirchhoff anisotropic shot migration is applied. Now, the turtle back structure is clearly visible in both images, and depth conversion is quite good. However, while the shot migration is excellent, several of the steeply dipping events are still misplaced.

Figure 7-16(e) compares isotropic shot and Kirchhoff migrations using the vertical velocity. There is no question that the shot migration is worth the effort, but neither of these migrations accurately image steeply dipping events.

Figure 7-16(f) shows why anisotropic imaging is worth the effort. The left hand side of (f) shows anisotropically imaged CDP's, while the right hand side shows isotropically imaged CDP's. The middle image is just a representation of the location of the CDP's at the top of the turtle-like structure. The greater flatness, along with improved amplitude response of the anisotropic CDP's, is clear evidence of the need to utilize anisotropic methods when available.